Sensors and Materials, Vol. 25, No. 3 (2013) 205–217
MYU Tokyo

S & M 0914

Growth of $Al_xGa_{1-x}N$ Structures on 8 in. Si(111) Substrates

Balakrishnan Krishnan*, Seungjae Lee, Hongwei Li,
Jie Su, Dong Lee and Ajit Paranjpe

Veeco MOCVD Operations, 394 Elizabeth Avenue, Somerset, NJ 08873, USA

(Received October 10, 2012; accepted February 20, 2013)

Key words: MOCVD, GaN, $A_xGa_{1-x}N$, Si substrate, wafer curvature

Device-oriented GaN layers have been grown with $Al_xGa_{1-x}N$ buffer structures as a bottom layer on 8 in. Si substrates using a commercial high-throughput metal organic chemical vapor deposition (MOCVD) system. The effect of the V/III ratio on the growth of AlN nucleation layers formed directly on Si(111) substrates has been analyzed. The effects of parasitic reactions between the group III precursor and ammonia have been observed to be a major stumbling block in achieving a high growth rate with better crystalline quality of AlN layers on Si(111) substrates. In addition, the effect of the growth rate of strain-relieving $Al_xGa_{1-x}N$ buffer structures on the wafer curvature of GaN structures during growth has been studied. It was found that the rapid growth of $Al_xGa_{1-x}N$ buffer structures helps reduce wafer bowing in GaN grown on top of the buffer structures.

1. Introduction

Group III nitride semiconductors are widely used in full-color display, liquid crystal displays, backlighting, mobile platforms, illumination, sensors, and detectors.[1–3] Recently, AlN thin films have become of great interest in micro- and nano-electromechanical systems (MEMS and NEMS) for sensing applications, which include biological sensing. In an undoped state, AlN acts as an insulator (electrical resistivity 10^{13} Ω·cm); therefore, it is used in a metal-insulator semiconductor structure in some hydrogen-sensing applications.[4,5] AlN is also a good candidate for sensing applications that require operation under extreme conditions because it has the largest energy gap among the group III nitride semiconductors (6.2 eV compared with 3.4 eV for GaN, 0.7 eV for InN, and 1.1 eV for Si).[6] Epitaxially grown AlN has a high surface acoustic wave (SAW)

*Corresponding author: e-mail: bkrishnan@veeco.com

velocity (5910 m/s), a moderate electromechanical coupling coefficient (approximately 1.0%), and a linear temperature coefficient.[7–9]

Most of the group-III-nitride-based materials and devices for commercial applications are grown on sapphire substrates owing to the lack of high-quality native bulk substrates. However, sapphire is too stable and difficult to micromachine. Also, there are major problems with sapphire when the substrate size is scaled up to 8 in. diameter or more owing to wafer bowing caused by lattice and thermal mismatch. The fabrication of vertically conducting devices of group III nitride semiconductors grown on sapphire is cumbersome and expensive. For these reasons, major research efforts are under way to develop group-III-nitride based optical and power device structures on Si(111) substrates. Group III nitride structures on silicon offer very attractive potential in terms of manufacturability and cost for many optoelectronic and microelectronic devices. In spite of these advantages, silicon has not been the most preferred material as a substrate for group III nitride semiconductors owing to several problems mainly related to cracking of the films due to excessive stress related to thermal and lattice mismatch. For the successful device-oriented growth of group III nitride structures on Si(111) substrates, wafer curvature due to thermal and lattice mismatch during the growth process must be controlled so as not to exceed a certain threshold using methods such as strain-relieving structures. In order to achieve high-yield device structures on 8 in. Si substrates, GaN thickness uniformity should be at least 3% or better with zero edge exclusion. Unlike sapphire, GaN cannot be grown directly on Si owing to the formation of eutectic Ga-Si and the associated meltback etching of Si substrates.[10] This necessitates the use of AlN as a starting mask material to facilitate the subsequent growth of group-III-nitride-based structures on Si substrates. When the growth is started with an AlN nucleation layer, it is difficult to grow thick GaN with the high structural quality required for device structures directly on top of the AlN without cracks, particularly when large substrates are used. Hence, a combination of $Al_xGa_{1-x}N$ buffer structures needs to be grown between the AlN nucleation layer and the GaN layer when a Si substrate is employed to reduce the lattice-mismatch-related stresses that built up in the structure. Compressive stress builds up during the growth of $Al_xGa_{1-x}N$ and GaN layers due to lattice mismatch. There have been various procedures and material combinations employed for the buffer growth.[13–16] It must be ensured that the lattice-mismatch-induced compressive stress matches the tensile stress in the structure after the completion of GaN growth while it is cooled to room temperature to prevent cracking in the structure. The accumulation of tensile stress is due to the difference in the thermal expansion coefficients between GaN and Si. The important lattice and thermal parameters of GaN, AlN, Si(111), and sapphire are given in Table 1. It must be mentioned that the thermal expansion coefficients of sapphire, GaN, and AlN correspond to the lateral planes in the direction normal to the c-axis. In this article, a systematic analysis of AlN and related structures grown on 200 mm (8 in.) Si(111) substrates using a commercial metal organic chemical vapor deposition (MOCVD) system is given. The dependence of the AlN structural quality and growth rate on the V/III ratio has been studied. The difference in AlN growth on Si(111) in comparison with sapphire-based growth is highlighted. In addition, the effect of the growth rates of the AlN nucleation layer and strain-relieving $Al_xGa_{1-x}N$ buffer layers on the wafer

Table 1
Lattice and thermal properties of GaN, AlN and the two prominent substrate materials, Si(111) and sapphire.

Material	Lattice parameter		Thermal conductivity ($W \cdot cm^{-1}K^{-1}$)	Thermal expansion coefficient in-plane ($10^{-6}K^{-1}$)	Lattice mismatch with GaN (%)	Thermal mismatch (%)
	a (Å)	*c* (Å)				
Si(111)	5.430	—	1.49	2.59	−16.9	54
Sapphire	4.758	12.991	0.5	7.5	16.0	−34
AlN	3.112	4.980	2.85	4.2	2.4	25
GaN	3.189	5.185	1.3	5.59	—	—

curvature of the GaN structure has been studied. The GaN structures were characterized by different methods specified in the experimental section of this article to determine whether a difference in the growth rate at the buffer level affects the structure and morphology of the structures.

2. Experimental

Device-oriented GaN structures were grown using a Veeco Turbodisc K465i MOCVD system. High-purity sources of trimethyl aluminum (TMAl), trimethyl gallium (TMGa), and ammonia (NH_3) were used as the precursors. The temperature was monitored and controlled at multiple points on the wafers using an *in situ* wafer surface temperature measurement system (RealTemp). The chamber wall, cold plate, and shower head were kept at a constant temperature of 50°C. The growth rate and wafer curvature were continuously measured all through the growth *in situ*. The system pressure was kept constant at 75 Torr to reduce the amount of parasitic reactions between the alkyl source (TMAl) and ammonia. The Si(111) substrates used for this study were of 8 in. (200 mm) diameter and 1 mm thickness and were single-side-polished. Figure 1 shows the typical GaN structure used in this study.

The substrates were first thermally cleaned under hydrogen atmosphere at a temperature of 1100°C for 3 min prior to the initiation of growth to remove organic impurities and oxide layers present on the surface of the substrates. In order to prevent temperature-influenced Si desorption from the surface and Si_xN_y formation due to the direct exposure of Si to ammonia, Al metal was deposited at a low temperature to mask the substrate surface. After the completion of the Si masking process, the temperature was raised to 1050°C to initiate the growth of an AlN nucleation layer of 130 nm thickness. This was followed by the growth of three layers of $Al_xGa_{1-x}N$ with three different Al molar fractions as shown in Fig. 1, with thicknesses of 200, 250, and 300 nm. These buffer layers are used to build up compressive stress in the structure. On top of the $Al_xGa_{1-x}N$ buffer structures, a 2.5 μm layer of undoped GaN was grown. To prevent the cracking of the GaN layer, a low-temperature AlN buffer layer of 80 Å thickness was inserted during the GaN growth. All the layers grown were characterized by X-ray diffraction (XRD), optical microscopy, and atomic force microscopy (AFM).

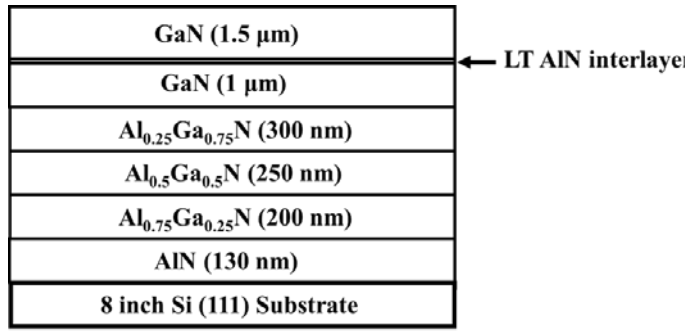

Fig. 1. GaN structure with AlN nucleation layer and strain-relieving $Al_xGa_{1-x}N$ layer on 8 in. Si(111) substrate.

For the analysis of AlN growth, an independent set of experiments was conducted on 8 in. Si(111) substrates. Thermal annealing of the substrates and the initial deposition of Al metal were carried out in the same way as described above. AlN layers with a constant thickness of 300 nm were grown under different V/III ratios by changing the ammonia flow. The growth temperature, measured at the wafer surface, was kept constant at 1050°C. In one of the AlN growth evaluation processes, the dependences of the structure and morphology on the V/III ratio were studied. The ammonia flow was varied from 50 to 2000 while keeping the TMAl flow constant.

3. Results and Discussion

3.1 *AlN growth analysis*

Figure 2 shows the dependence of the AlN growth rate on the ammonia flow. Here, it must be emphasized that the TMAl flow is kept constant and, hence, the V/III ratio is changed by varying the ammonia flow only. As shown in Fig. 2, the growth rate increases with decreasing ammonia flow owing to the decrease in the amount of parasitic reactions. In addition, the surface morphology and structural quality of the AlN layers were observed to improve with the reduction of the ammonia flow as evidenced by microscopic and XRD analyses. Unlike the growth of AlN on sapphire substrates, the growth of high-structural-quality AlN on Si substrates is extremely difficult owing to temperature limitation of the process and the formation of Al-Si.[10] It is well established that in order to improve the structural quality of AlN, high-temperature growth must be employed owing to the inherent lack of lateral movement of aluminum species and the high sticking coefficient of Al of close to unity.[1,17,18] Because of its high sticking coefficient close to unity, aluminum tends to form only islands of AlN during growth after the reaction with NH_3. For good epitaxial growth, the source species must readily migrate on the surface so that they can attach to the lattice at energetically favorable sites as in the case of Ga species during the growth of GaN. In order to readily achieve

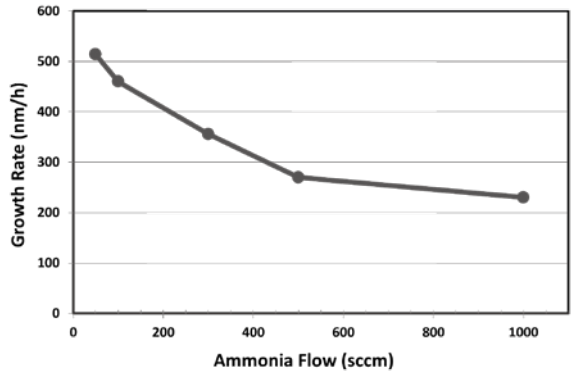

Fig. 2. Variation of growth rate of AlN layers with ammonia flow at constant growth temperature and TMAl flow.

this in the case of AlN, one of the most effective methods is to perform the growth at temperatures of more than 1250°C, which imparts sufficient energy to the Al atoms and thus enables them to move in the lateral direction. However, this method is feasible only when substrates such as sapphire are employed for growth. In the case of Si, the required temperature cannot be readily used owing to the desorption of Si atoms from the substrate surface and subsequent roughening. Even if the surface is covered with metallic aluminum during the initiation of growth, a subsequent increase in temperature causes pits to form on the growing AlN surface. With the decrease in V/III ratio, the density of pits decreases monotonically, clearly showing that the coalescence increases and the surface morphology consequently improves. The major reason for these improvements is the reduced amount of parasitic reactions in the system. The parasitic reactions not only cause the loss of species available for growth, but also increase the number of nanometer-size particles in the chamber. The particles formed during the parasitic reactions constantly fall on the growing surface and form additional nucleation sites. This increases the amount of three-dimensional islands on the growing surface and the formed islands do not coalesce easily owing to the temperature restriction and the lack of the required Al species. The damage to the Si substrate surface during the initiation of high-temperature AlN growth and the insufficient coalescence of the AlN textures formed result in a surface with a high pit density as evidenced by the AFM images shown in Figs. 3(a)–3(e). However, with decreasing ammonia flow, the growing surface receives more Al metal species, and this helps improve coalescence, thus reducing the pit density on the surface. A high-resolution TEM cross-sectional analysis performed on an AlN sample grown in this series showed the presence of an amorphous phase containing Si-Al and Si_xN_y. This amorphous coating acts as a shield to prevent the direct reaction between the Si surface and ammonia. However, during the subsequent increase of temperature to grow AlN, part of this amorphous phase formed tends to

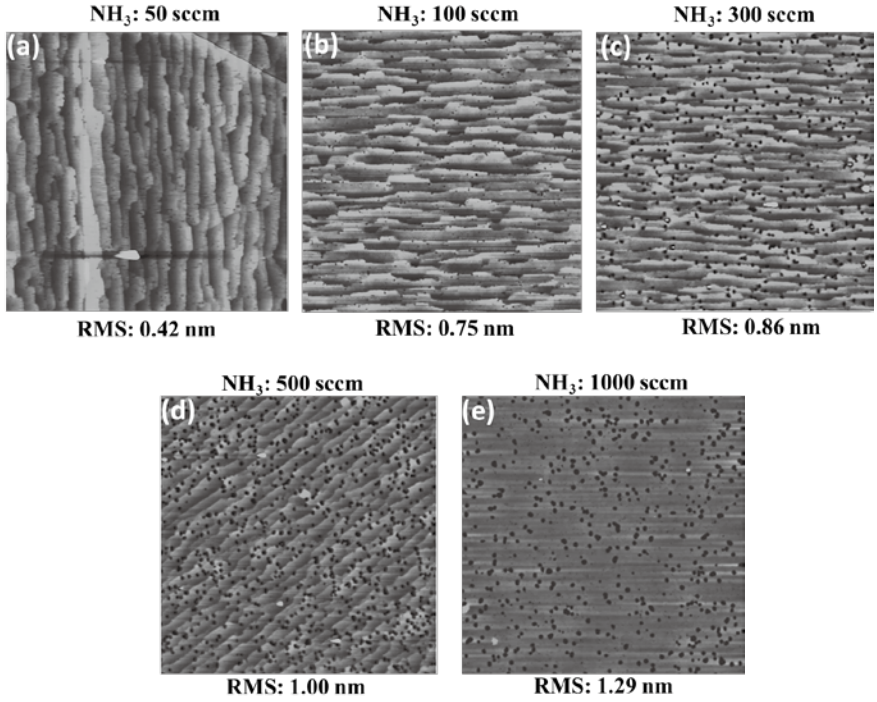

Fig. 3. AFM surface morphologies (5 × 5 μm^2) of AlN layers grown under different ammonia flow conditions.

crystallize due to the influence of increasing atomic nitrogen supply from ammonia and temperature. This tends to expose scattered parts of the Si surface to source species and the formation of Si-Al eutectic or Si_xN_y to a less extent, especially considering the pits formed on the AlN surface as seen in the AFM images.[19] This kind of substrate-influenced pit formation is not observed commonly when sapphire is used. The AlN layer grown with just 50 sccm of ammonia has an almost pit-free surface with a step growth feature. Normally, a step growth feature appears only when the growth is two dimensional. However, the layer grown with a 50 sccm flow of ammonia is cracked owing to the accumulation of tensile strain in it and its better structural quality. The higher the structural quality of the AlN layer, the more rapidly it forms cracks when it is directly grown on a Si(111) substrate owing to the large lattice mismatch of 23.4%.[20] It was observed that the thickness of crack-free AlN that can be grown on Si(111) increases with the increase in the V/III ratio used for the growth. The structural quality and surface morphology must be compromised to increase the thickness of crack-free AlN. The lattice-mismatch-influenced strain is adequately accommodated in the lattice by the defects formed during the growth process, and hence, no cracks are formed. The XRD

(0001) on-axis ω FWHM values measured for the AlN layers grown with ammonia flows of 50, 100, 300, 500, and 1000 sccm were, respectively, 796, 871, 910, 956, and 998 arcsec. These are impressive values considering that the thickness of AlN is only 0.3 μm and the substrate employed is 8 in. Si(111).

3.2 *Effect of $Al_xGa_{1-x}N$ buffer structure growth rate on wafer curvature*

The wafer curvature is an extremely important characteristic of GaN/Si-based structures, which must to be controlled along with the lattice-misfit-generated dislocations in order to successfully commercialize this technology for use with GaN/sapphire-based devices. There are major efforts being undertaken to grow thick and crack-free GaN layers as part of the efforts to accomplish high-performance optoelectronic and electronic device structures. Several intermediate buffer structures including superlattices are now being used as strain-relieving layers between GaN and the Si(111) substrate. One of the simplest approaches is to use bulk $Al_xGa_{1-x}N$ layers of different compositions and thicknesses as used in the present investigation (Fig. 1). The growth rate is one of the various tuning parameters for nucleation and strain-relieving layers used to optimize the GaN structure growth process. In the GaN/Si structure presented in Fig. 1, the growth rates of AlN and the strain-relieving $Al_xGa_{1-x}N$ buffer were varied to determine any change in wafer curvature at different stages. The tensile strain, generated during the cooling process, is mainly due to the difference in the thermal expansion coefficient between the GaN epilayers and the Si(111) substrate during the cooling process. Figure 4 shows the change in the wafer curvature recorded during the growth of GaN/Si

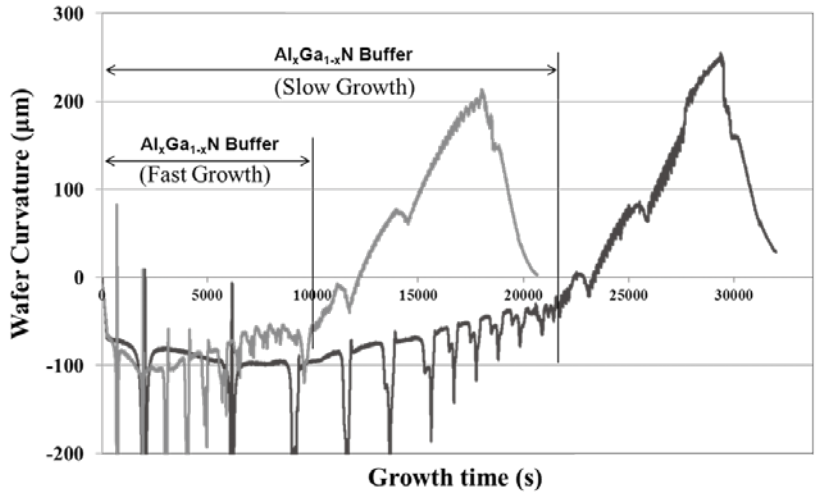

Fig. 4. Variation of wafer curvature during different stages of GaN/Si structure growth with (a) high growth rates of AlN nucleation layer and $Al_xGa_{1-x}N$ strain-relieving layers and (b) low growth rates.

structures with high and low rates of growth for the AlN nucleation and $Al_xGa_{1-x}N$ buffer layers. As shown in the figure, the resultant GaN structure grown with a low rate of growth of the nucleation layers has a room-temperature wafer convex curvature of +30 μm, which means that the wafer is still compressively stressed. On the other hand, the structure grown at a high rate has a room-temperature wafer curvature of zero. This indicates that the wafer is flat and ideally suited for further device processing from the viewpoint of the wafer curvature requirement although the structure itself requires further device components on top of the GaN. A possible reason for the change in strain in the structure is the change in the coalescence pattern in the grains of the AlGaN and GaN films. This shows that the stress can be managed by balancing the growth rate and coalescence behavior of the grains in the structure. This is supported by the observation that the structural and morphological characteristics of the most important GaN layer on top of the buffer structures grown at high and low rates exhibited almost identical behavior. Figure 5(a) shows the AFM surface morphology (5×5 μm^2) of the GaN layer grown on top of the rapidly grown buffer structure. This is a typical GaN/Si pattern with an AFM root mean square (RMS) index of 0.15 nm. The corresponding AFM surface morphology of the slowly grown structure is given in Fig. 5(b), and the RMS index of this layer was measured to be 0.17 nm. The GaN XRD on-axis (0002) FWHM values of the layers were 259 and 279 arcsec, respectively, which are not significantly different. The reason why the buffer structure grown with a low growth rate resulted in larger wafer bowing may be due to the difference in the grain-coalescence-related phenomenon at the molecular level. When $Al_xGa_{1-x}N$ layers are kept under the growth conditions for a long period of time, the Ga species in the grains tend to diffuse in the lateral direction. Although this is better purely from an epitaxial point of view as it improves the structural quality of the $Al_xGa_{1-x}N$ film, the improved grain coalescence increases the effective stress in the layers and, hence, increases the effective compressive stress. On the other hand, when the $Al_xGa_{1-x}N$ buffer layers are grown at a higher growth rate, owing to the insufficient time to complete the coalescence, voids remain buried in the films. These nanometer-size point defects help absorb the stress in the structure better and, hence, the

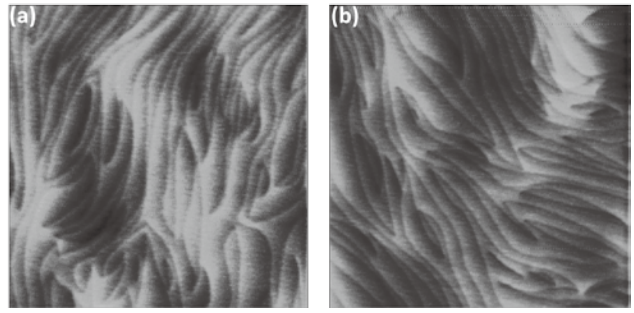

Fig. 5. AFM surface morphologies (5×5 μm^2) of GaN layers grown on (a) rapidly grown and (b) slowly grown $Al_xGa_{1-x}N$ buffer structures.

wafer curvature is reduced. Since the defects are in the $Al_xGa_{1-x}N$ layers, they should have less effect on the device characteristics.

Another important observation made for the wafers is the difference in the coalescence-influenced surface morphology at the edge of the film structure. Figure 6 shows optical microscopy images of GaN surfaces grown on top of the rapidly and slowly grown $Al_xGa_{1-x}N$ buffer structures. The images in Fig. 6 show the surface morphologies of the GaN structures at the center of the wafers. No difference can be seen in the morphologies. However, at the edge of the wafers, the surface morphologies showed distinct differences. The GaN structure grown on the rapidly grown buffer structure had a surface morphology at the edge that was identical to the other regions of the wafer as shown in Fig. 6(c). This indicates that the grown GaN is completely coalesced, resulting in a smooth surface over the entire 8 in. substrate. Figure 6(d) shows an optical microscopy image of the wafer edge in the case of GaN formed on the slowly grown AlGaN buffer structure. There are many dark regions in this image and lattice cracks are also visible behind the dark regions. The dark regions are the result of Ga meltback etching of the Si substrate initiated by the flow of Ga to the bottom through the lattice cracks generated at the edge of the wafer grown with the slowly grown $Al_xGa_{1-x}N$ structure. When the $Al_xGa_{1-x}N$ buffer layers are grown at a low rate, the Ga component of the AlGaN lattice undergoes diffusion in the rough $Al_xGa_{1-x}N$ grains formed on AlN.

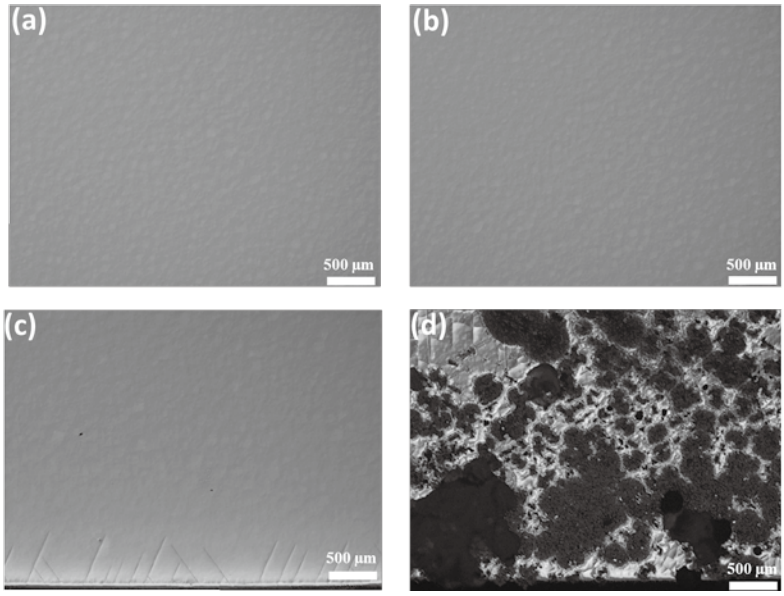

Fig. 6. Optical microscopy images of GaN surface recorded at the wafer (a) center and (c) edge with rapidly grown AlGaN and AlN bottom layers; (b) center and (d) edge with slowly grown AlGaN and AlN bottom layers.

Subsequently, coalescence between the grains takes place at a lower rate. Most of the wafer is supplied with stoichiometric amounts of aluminum and gallium species along with ammonia. However, at the edges of the wafer, owing to the presence of the wafer pocket edge, a difference in flow is caused. This forces an increase in the supply of Ga at the edges owing to a reduction of temperature of up to a maximum of 5°C. With the progress of epitaxial growth, Ga diffuses and forms $Al_xGa_{1-x}N$ crystallites of better structural quality. $Al_xGa_{1-x}N$ buffer structures of high structural quality cannot withstand the stress generated by the lattice mismatch, in contrast to the partially coalesced layers. This causes cracks in the $Al_xGa_{1-x}N$ layers at the edge. When GaN is deposited on top of the thicker $Al_xGa_{1-x}N$ buffer layers, the $Al_xGa_{1-x}N$ layers at the bottom cannot withstand the stress and, hence, start cracking. The formed cracks form a pathway for Ga species to reach the Si substrate beneath and initiate the meltback etching process. This problem can be overcome by calculating the flows at different regions corresponding to the temperatures and making corrections accordingly.

4. Summary

A systematic analysis has been performed on two aspects of GaN/Si structure growth employing 8 in. Si (111) substrates. In the first study, the effect of parasitic reactions on the structural and morphological properties of AlN with increasing ammonia flow was investigated at a constant growth temperature and TMAl source flow. The effect of the growth rate variation of the AlN nucleation layer and the $Al_xGa_{1-x}N$ buffer layers on the GaN/Si structure was analyzed in the second study. In the AlN growth, the growth rate, structural quality, and morphology were affected by the V/III ratio used. With increasing ammonia flow, and hence, the V/III ratio, the AlN growth rate decreased and the corresponding structural and morphological qualities became poorer. A pitless AlN surface with the narrowest XRD (0002) on-axis FWHM value of 798 arcsec among the layers analyzed was measured for the layer grown with the lowest ammonia flow of 50 sccm. In the analysis of the GaN/Si structure, it was found that the growth rate variation did not affect the structural and morphological qualities of GaN. However, the wafer curvature of the GaN structure was lower when a high growth rate was used for AlGaN buffer layers and the AlN nucleation layer. In addition, $Al_xGa_{1-x}N$ layers prepared with a low growth rate resulted in lattice-cracked layers and, as a consequence, paved the way for Si substrate meltback etching by Ga at the edge of the wafers. On the basis of the the results, it can be concluded that the rapid growth of $Al_xGa_{1-x}N$ buffer structures helps reduce wafer bowing in GaN grown on top of the buffer structures.

References

1 A. Khan, K. Balakrishnan and T. Katona: Nat. Photonics **2** (2008) 77.
2 H. Morkoc: Handbook of Nitride Semiconductors and Devices, Vol. 1 (Springer, Berlin, 2007).
3 S. Pimputkar, J. S. Speck, S. P. DenBaars and S. Nakamura: Nat. Photonics **3** (2009) 180.
4 E. F. Mccullen H. E. Prakasam, W. Mo, R. Naik, K. Y. S. Ng, L. Rimai and G. W. Auner: J. Appl. Phys. **93** (2003) 5757.

5 F. Serina, K. Y. S. Ng, C. Huang, G. W. Auner, L. Rimai and R. Naik: Appl. Phys. Lett. **79** (2001) 3350.
6 B. G. Streetman and S. Banerjee: Solid State Electronic Devices, 5th ed. (Prentice Hall, New Jersey, 2000).
7 H. Guopeng, J. Xu, G. W. Auner, J. Smolinski and H. Ying: Sens. Actuators, B **132** (272) 2008.
8 T. Suetsugu, T. Yamazaki, S. Tomabechi, K. Wada, K. Masu and K. Tsubouchi: Appl. Surf. Sci. **117/118** (1997) 540.
9 K. Tsubouchi and N. Mikoshiba: IEEE Trans. Sonics Ultrason. **SU-32** (1985) 634.
10 M. K. Sunkara, S. Sharma, R. Miranda, G. Lian and E. C. Dickey: Appl. Phys. Lett. **79** (2001) 1546.
11 A. V. Lobanova, K. M. Mazaev, R. A Talalaev, M. Leys, S. Boeykens, K. Cheng and S. Degroote: J. Cryst. Growth **287** (2006) 601.
12 T. G. Mihopoulos, V. Gupta and K. F. Jensen: J. Crystal Growth **195** (1998) 733.
13 S. Lawrence Selvaraj, A. Watanabe and T. Egawa: Appl. Phys. Lett. **98** (2011) 252105.
14 P. Chen, R. Zhang, Z. M. Zhao, D. J. Xi, B. Shen, Z. Z. Chen, Y. G. Zhou, S. Y. Xie, W. F. Lu and Y. D. Zheng: J. Cryst. Growth **225** (2001) 150.
15 E. Feltin, S. Dalmasso, P. de Mierry, B. Beaumont, H. Lahrèche, A. Bouillé, H. Haas, M. Leroux and P. Gibart: Jpn. J. Appl. Phys. **40** (2001) L738
16 F. Jiang, W. X. Wangli, W. Fang, C. Mo, J. Liu, Y. Tang, C. Xiong, H. Cheng, C. Zheng, Y. Zhou, Z. Yan and L. Bo: Compd. Semicond. June **21** (2010).
17 K. Balakrishnan, A. Bandoh, M. Iwaya, S. Kamiyama, H. Amano and I. Akasaki: Jpn. J. Appl. Phys. **46** (2007) L307.
18 M. Imura, K. Nakano, G. Narita, N. Fujimoto, N. Okada, K. Balakrishnan, M. Iwaya, S. Kamiyama, H. Amano, I. Akasaki, T. Noro, T. Takagi and A. Bandoh: J. Cryst. Growth **298** (2007) 257.
19 G. Radtke, M. Couillard, G. A. Botton, D. Zhu and C. J. Humphreys: Appl. Phys. Lett. **100** (2012) 011910.
20 K. Y. Zang, L. S. Wang, S. J. Chua and C. V. Thompson: J. Cryst. Growth **268** (1004) 515.

About the Authors

Balakrishnan Krishnan is a Senior Research Scientist at Veeco MOCVD operations in New Jersey, USA. After earning his Ph.D. in Semiconductor Physics (Crystal Growth and Characterization) from Anna University, India, in 1992, he moved to Japan and did extensive research on III-nitride & III-V epitaxy and devices until March 2007. From April 2007 until 2010, he was a Research Professor at the University of South Carolina, and during this period, he continued to focus on MOCVD growth of nitride semiconductors and devices. He is the author of 142 journal publications, several book chapters, and about 256 conference presentations (including 20 invited lectures). He was a principal Investigator/ Coinvestigator of several research projects related to III-V and III-nitride layer growth, characterization, and device fabrication. He is a reviewer of several technical journals and is a member of many professional societies including Materials Research Society and American Association for Crystal Growth.

Seung-Jae Lee received his B.S. and M.S. degrees in advanced materials engineering, and the Ph.D. degree from the Department of Information and Electronic Materials Engineering from Chonbuk National University, Jeonju, Korea, in 2001, 2003, and 2011, respectively. From 2005 to 2011, he was a Senior Researcher at Korea Photonics Technology Institute, Gwangju, Korea. He is currently a postdoctoral senior research scientist at Veeco Instruments Inc., Somerset, New Jersey. His research interests include the growth of semiconductor materials and their electronic and photonic device applications.

Hongwei Li is a Research Scientist at Veeco MOCVD Operations since 2008. He is working on the MOCVD growth and characterization of AlInGaN materials on Si substrates for both high-electron-mobility transistors and light-emitting diodes. He received his Ph.D. degree in Chemical Engineering from the University of Louisville in 2005.

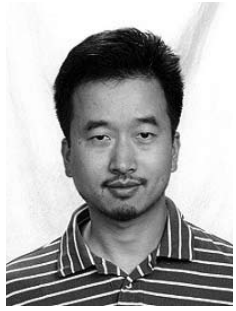

Jie Su is a Senior Staff Scientist at Veeco MOCVD Operations at Somerset, New Jersey. He is working on AlGaInN epitaxy on Si for both high-electron-mobility transistors and light-emitting diodes using the MOCVD system. He was a technologist at Applied Materials at Santa Clara, CA from 2006–2011. He authored and coauthored more than 15 journal articles, 3 book chapters, and more than 10 granted patents. He is a member of the Institute of Electrical and Electronics Engineers (IEEE), and the Scientific Research Society (Sigma Xi) from 2006. He received his M.S. and Ph.D. in Engineering and Applied Science from Yale University in 2005.

Dong S. Lee is the Director of Application at Veeco Instruments since 2006 with characterization, nitride LEDs, and GaN/Si crystal growth. He initiated the GaN/Si program in 2010, and has been leading the team since then. Prior to joining Veeco, Dr. Lee worked in the US Air Force Research Laboratory (AFRL) for 3 years. His work has been focused on semiconductor quantum-well devices for the FIRST project (Future IR Sensor Technology). He joined Emcore TurboDisc as an R&D lab manager in 1998, and he has worked on compound semiconductor epitaxy of solar cells, laser diodes, LEDs, photodetectors, and electronic device materials. He received his B.S. in Physics from Korea University in 1981, M.S. in Physics from Western Illinois University in 1988, and Ph.D. in physics

from University of New Mexico in 1995. He demonstrated the first gain without conversion in GaAs/InGaAs/AlGaN compound semiconductor QWs. Dr. Lee has been working on the research and development of III-V, III-N, and oxide materials using advanced characterizations and MOCVD crystal growth. His research interests are basic material growth with analysis and development of device-related materials. He is also interested in Creation Science.

Ajit Paranjpe is presently Sr. Vice President and Chief Technology Officer of Veeco. He has over twenty years of technology and senior management experience in the semiconductor and capital equipment industry. At Veeco, he has led the development of equipment and applications for the HB-LED, solar, and data storage markets. He joined Veeco from Media Lario where as VP for Lithography Products, he introduced high-precision collector optics for EUV lithography. Prior to Media Lario, Dr. Paranjpe served as VP for Marketing & Applications at Therma-Wave where he was responsible for their critical dimension, thin film, and implant/anneal metrology products. He joined Therma-Wave from TORREX. As CTO at TORREX, he led the development of their innovative CVD & ALD mini-batch tools. Earlier, he was Director of Process Technology at Veeco-CVC, Inc. where he managed process technology development and customer demonstrations for their PVD, CVD, and IBD/IBE products. He spent several years at Texas Instruments, where his technical responsibilities spanned process integration, process development, and equipment development for CMOS technology. He has broad experience related to the fabrication of semiconductor, opto-electronic, and magnetic thin film devices. Dr. Paranjpe has co-authored over 30 publications and holds 46 US patents. He is a member of AVS, ECS, and IEEE.